Cellular & Molecular Immunology (2018) 15, 120–134

www.nature.com/cmi

RESEARCH ARTICLE

Toxoplasma gondii GRA15$_{II}$ effector-induced M1 cells ameliorate liver fibrosis in mice infected with *Schistosomiasis japonica*

Yuanyuan Xie[1,7], Huiqin Wen[1,2,3,7], Ke Yan[4], Shushu Wang[5], Xuesong Wang[5], Jian Chen[1,6], Yuanling Li[1], Yuanhong Xu[1], Zhengrong Zhong[4], Jilong Shen[1,2] and Deyong Chu[1]

Recent studies indicated that type II *Toxoplasma gondii* (*Tg*) GRA15$_{II}$ favored the generation of classically activated macrophages (M1), whereas type I/III *Tg*ROP16$_{I/III}$ promoted the polarization of alternatively activated macrophages (M2). A number of studies have demonstrated that M2 cells are involved in the pathogenesis of the liver fibrogenesis caused by *Schistosoma japonicum*. The purpose of the present study was to explore the inhibitory effect of *Toxoplasma*-derived *Tg*GRA15$_{II}$ on mouse hepatic fibrosis with schistosomiasis. The *gra15*$_{II}$ and *rop16*$_{I/III}$ genes were amplified from strains *T. gondii* PRU and Chinese 1 Wh3, respectively. Lentiviral vectors containing the *gra*15$_{II}$ or *rop*16$_{I/III}$ plasmid were constructed and used to infect the RAW264.7 cell line. The polarization of the transfected cells was evaluated, followed by co-culture of the biased macrophages with mouse hepatic stellate JS1 cells. Then, mice were injected with GRA15$_{II}$-driven macrophages via the tail vein and infected with *S. japonicum* cercariae. *Tg*GRA15$_{II}$ induced a M1-biased response, whereas *Tg*ROP16$_{I/III}$ drove the macrophages to a M2-like phenotype. The *in vitro* experiments indicated that JS1 cell proliferation and collagen synthesis were decreased following co-culture with *Tg*GRA15$_{II}$-activated macrophages. Furthermore, mice inoculated with *Tg*GRA15$_{II}$-biased macrophages displayed a notable alleviation of collagen deposition and granuloma formation in their liver tissues. Our results suggest that *Tg*GRA15$_{II}$-induced M1 cells may dampen the M2 dominant pathogenesis of hepatic fibrosis and granulomatosis. These results provide insights into the use of parasite-derived immunomodulators as potential anti-fibrosis agents and to re-balance the schistosomiasis-induced immune response.
Cellular & Molecular Immunology (2018) **15,** 120–134; doi:10.1038/cmi.2016.21; published online 9 May 2016

Keywords: fibrosis; GRA15$_{II}$; ROP16$_{I/III}$; schistosomiasis; *Toxoplasma gondii*

INTRODUCTION

Schistosomiasis is a major chronic disease of humans in endemic regions. The formation of liver egg granulomas and hepatic fibrosis are the primary causes of morbidity and mortality in human schistosomiasis.[1] The continuous fibrogenic process of liver tissues after praziquantel therapy demonstrates the importance of developing new strategies against schistosomiasis.[2,3] The immune response of mice to *Schistosoma japonicum* infection progresses through at least three phases. A Th1-like response dominates when the animals are exposed to migrating schistosomula during the first 4 weeks post infection. A Th2-like response gradually becomes apparent 1–2 weeks later; this response is primarily triggered by the soluble egg antigens produced by mature miracidia. The skewed response reaches its peak ~8 weeks post infection, resulting in acute symptoms in patients.[4,5] Then, the Th2 response is downregulated and the newly formed granulomas shrink during the chronic stage at week 12.[6] Thus, the Th2 response promotes gene transcription pathways associated with granuloma formation and collagen synthesis.[4]

[1]Department of Pathogen Biology, Provincial Laboratories of Pathogen Biology and Zoonoses Anhui, and Clinical Laboratory of the First Affiliated Hospital, Anhui Medical University, Hefei 230022, China; [2]Department of Immunology, Anhui Medical University; Hefei 230022, China; [3]Department of Blood Transfusion, The First Affiliated Hospital of Anhui Medical University, Hefei 230022, China; [4]Department of Laboratory Diagnosis, The Affiliated Hospital of Bengbu Medical College, Bengbu, Anhui 233004, China; [5]Pediatrics Department of Affiliated Provincial Hospital, Anhui Medical University, Hefei 230001, China and [6]Intensive Care Unit of Affiliated Provincial Hospital, Anhui Medical University, Hefei 230001, China
[7]These authors contributed equally to this work.
Correspondence: Dr Professor J Shen or Dr Associate Professor D Chu, Department of Pathogen Biology, Provincial Laboratories of Pathogen Biology and Zoonoses Anhui, and Clinical Laboratory of the First Affiliated Hospital, Anhui Medical University, Hefei, 230022, China.
E-mail: shenjilong53@126.com or chudeyong@126.com
Received: 24 November 2015; Revised: 5 February 2016; Accepted: 8 March 2016

Recent studies indicated that hepatic macrophages were the main cellular components of granulomas and had an important role in host immune responses to schistosome infection.[6–8] Macrophages have the capability to promote, restrict or resolve inflammation and fibrosis depending on their activation state.[8–10] Two distinct states of polarized macrophage activation that mirror Th1–Th2 lymphocyte polarization have been recognized. The classically activated macrophage phenotype (M1) is activated by inflammatory cytokines such as interferon (IFN)-γ and is associated with the differentiation of Th1 cells. M1 macrophages produce inducible nitric synthase (iNOS), which helps generate the strong pathogen killing factor nitric oxide (NO).[11] In contrast, the alternatively activated macrophage phenotype (M2) is induced by Th2 cytokines such as interleukin (IL)-4 and IL-13[12,13] and is characterized by high arginase-1 (Arg-1), macrophage mannose receptor and chitinase-like molecule (Ym1) expression.[14,15] The shaping of macrophage functions is essential for host resistance to pathogens, tissue damage and repair. L-Ornithine, which is a major product of arginase catalysis, is a precursor for the production of polyamines and proline that favor cell proliferation and collagen production, respectively.[6,16,17] However, L-arginine may also be oxidized by iNOS to L-citrulline and NO, which may inhibit the collagen synthesis process.[18,19] Thus, the data strongly suggest that M1 macrophages are favorable for the amelioration of fibrosis through NO production.[20,21] Switching of macrophage functions from repair to killing during chronic schistosomiasis is likely critical when confronting the process of liver fibrosis.[22]

Toxoplasma gondii is a highly successful obligatory intracellular parasite that is capable of infecting almost all warm-blooded animals including humans and affects nearly 30% of the world population.[23,24] *T. gondii* infection is usually asymptomatic in healthy adults but can cause lethal toxoplasmosis in immunocompromised individuals.[25,26] *Toxoplasma* may establish a lifelong chronic infection in the host by evading and subverting the host immune system. *T. gondii* secretes essential effector molecules from secretory organelles, rhoptries, dense granules and micronemes into the host cytosol that modulate host signaling pathways and dictate virulence.[27–31] Among them, dense granule protein 15 (GRA15) and rhoptry kinase 16 (ROP16) have less dramatic but significant effects on virulence in mice and significantly alter host cell transcription.[29,31–33] Effector polymorphism-associated studies have shown that mouse macrophages infected with type II *Toxoplasma* induce M1 cell activation, whereas macrophages infected with type I or III *Toxoplasma* are polarized toward an M2 state. This difference is due to polymorphisms in $GRA15_{II}$ and $ROP16_{I/III}$, which activate STAT6/STAT3 signaling and nuclear factor (NF)-κB, respectively.[33] Interestingly, we found that *Toxoplasma*-type Chinese 1 strains possessed both $GRA15_{II}$ and $ROP16_{I/III}$ polymorphic effectors.[34,35]

In the present study, we infected the mouse macrophage RAW264.7 cell line with lentiviral vectors containing the $gra15_{II}$ or $rop16_{I/III}$ gene to drive macrophage polarization towards M1 or M2, respectively. The *gra*15 and *rop*16 genes were amplified from the PRU (type II) and Wh3 (Chinese 1) strains, respectively. $GRA15_{II}$- and $ROP16_{I/III}$-induced M1 and M2 macrophages were co-cultured with the mouse hepatic stellate JS1 cell line in transwells to verify the *in vitro* effect of the skewed macrophage phenotype on fibroblast activation and proliferation and collagen production. Additionally, the mice were treated with activated M1 cells via high-pressure injection of the tail vein followed by infection with schistosome cercariae and the pathology of liver granulomatosis and fibrosis were explored.

MATERIALS AND METHODS

Materials

Puromycin (PM), penicillin, streptomycin, phorbol 12-myristate 13-acetate, the hematoxylin and eosin (HE) staining kit, the Masson trichrome staining kit, ionomycin, transforming growth factor beta 1 (TGF-β1) antibody and flag-tag antibody were purchased from Sigma (St. Louis, MO, USA). Dulbecco's modified Eagle's medium, fetal bovine serum (FBS), Roswell Park Memorial Institute 1640 medium (RPMI 1640) and Hank's balanced salt solution were obtained from Wisent (Montreal, QC, Canada). Protease inhibitors, phenylmethanesulfonyl fluoride, the BCA protein assay kit, SDS-polyacrylamide gel electrophoresis and Red Blood Cell Lysis buffer were purchased from Beyotime (Shanghai, China). Radio-immunoprecipitation assay lysis buffer and nitrocellulose membranes were obtained from Millipore (Billerica, MA, USA). Antibodies against iNOS, Arg-1, matrix metalloproteinase 13 (MMP13), α-smooth muscle actin (α-SMA), type 1 collagen (Col I) and glyceraldehyde-3-phosphate dehydrogenase (GAPDH) for western blotting were purchased from Proteintech (Chicago, IL, USA). Antibodies against α-SMA and TGF-β1 were obtained from Abcam (Cambridge, MA, USA). Col I and MMP13 were manufactured by Bioworlde (Louis Park, BD, USA) for immunohistochemistry (IHC) analysis. Enzyme-linked immunosorbent assay (ELISA) kits for α-SMA, iNOS, Arg-1, MMP13 and hyaluronic acid (HA) were obtained from CUSABIO (Wuhan, China), and cytokine kits were obtained from R&D Systems (Minneapolis, MN, USA).

Parasites

T. gondii tachyzoites from Wh3 (type Chinese 1) and PRU cysts (type II) were harvested from a laboratory mouse passage on days 3 and 30 post infection, respectively. Snails (*Oncomelania hupensis*) infected with *S. japonicum* were provided by the Jiangsu Institute of Parasitic Disease Control (Wuxi, China).

Plasmid construction and lentivirus infection

Amplification of the open reading frame encoding $Tg GRA15_{II}$ (lacking the signal peptide, 1500 bp, ToxoDB.org) and $Tg ROP16_{I/III}$ (2124 bp, ToxoDB.org) was achieved through real-time (RT)-PCR from the whole PRU strain cyst RNA and Wh3 tachyzoite RNA, respectively. The primers were as follows: for $gra15_{II}$, forward 5′-CGCTCGAGAATAATTCGGTGGCTTG-3′ (the *Xho*I site is underlined) and reverse 5′-AGGGATCCTTCATGGAGTTACCGCTGATTG-3′ (the *Bam*HI site is

underlined) and for $rop16_{I/III}$, sense 5′-GAATTCATGAAA GTGACCACGAAAG-3′ and antisense 5′-GGGTACCCTAC ATCCGATGTGAAGAAAGTT-3′ (the *Eco*RI and *Kpn*I sites are underlined, respectively). Primer synthesis and gene sequencing were completed by Sangon Biotech (Shanghai, China). The plasmid vector pEGFP-C2 (BD Biosciences, Franklin Lakes, NJ, USA) was utilized to generate mammalian expression constructs carrying $gra15_{II}$ or $rop16_{I/III}$. PCR-generated fragments were directionally cloned into the pEGFP-C2 vector, and the recombinant plasmids were transformed into *Escherichia coli* DH5α. The recombinant lentiviruses lentiviral vectors (LV)-pEGFP-$gra15_{II}$ and LV-pEGFP-$rop16_{I/III}$ contained the Flag tag (GeneChem Co., Shanghai, China).

Cells and co-culture system

The mouse hepatic stellate JS1 cell line was a gift from Dr Jinsheng Guo from Shanghai Zhongshan Hospital (FuDan Univ Div Digest Dis, China). The RAW264.7 cell line was purchased from the American Type Culture Collection (Manassas, VA, USA). Recombinant lentivirus plasmids were transfected into RAW264.7 cells (empty LV was used as the control), and stable transfectants were selected with PM according to the manufacturer's instructions. The three transfected cell lines were named $GRA15_{II}$-RAW264.7, $ROP16_{I/III}$-RAW264.7 and LV-RAW264.7 and were cultured in Dulbecco's modified Eagle's medium supplemented with heat-inactivated 10–15% FBS, 2 mM L-glutamine (Gibco, Grand Island, NY, USA), 100 U/ml penicillin and 100 μg/ml streptomycin. The JS1 cells were maintained in the same medium as the RAW264.7 cells except for the absence of L-glutamine. All cell cultures were maintained in incubators set at 37 °C with 5% CO_2. The cell lines were routinely assessed and confirmed to be free of *Mycoplasma* contamination.

A co-culture system was established using transwell inserts (Corning, Corning, NY, USA). Briefly, the bottom of the inserts was composed of polyester materials with a pore size of 0.4 μm, which permitted the passage of only small and soluble factors but not cells. Tansfected RAW264.7 and control RAW264.7 cells (1.5×10^6) were separately added to the upper well. JS1 cells (8×10^5) in the lower wells were co-cultured in a 6-well plate for the indicated time intervals. The co-culture system was maintained in 3 ml of basic culture medium supplemented with 10% FBS and 1% penicillin/streptomycin in 5% CO_2 at 37 °C. After co-culturing for 24 and 72 h, the JS1 cells were collected for total RNA and protein extraction.

Animal preparation and ethics statement

Six-week-old female BALB/c mice (17–20 g) were provided by the Changzhou Cavens Laboratory Animal Company, China (production permit number: Scxk 2011-003). The mice were maintained at a facility with a controlled temperature (20 ± 2 °C) and constant humidity (55 ± 5%) under a 12 h/12 h light/dark cycle with free access to food and water. All animal experiments were performed in strict accordance with the Chinese National Institute of Health Guide for the Care and Use of Laboratory Animals. All work was approved by the Institutional Review Board of the Institute of Biomedicine at Anhui Medical University (permit number: AMU 26-093628) and efforts were made to minimize the number of animals used and suffering during the experimental process.

The mice were randomly divided into four groups (12 mice per group) as follows: phosphate-buffered saline (PBS) control, $GRA15_{II}$-RAW264.7, LV-RAW264.7 and RAW264.7. Each mouse was infected percutaneously with 15 ± 2 schistosome cercariae 7 days after tail vein injection with treated cells (2×10^6 macrophages diluted in 150 μl PBS). The control mice were synchronously administered the same volume of PBS alone. All animals received a second injection on the day of parasite infection and were euthanized 56 days post infection with the schistosome cercariae.

Blood samples were incubated at 37 °C for 30 min and centrifuged for 10 min (1, 200*g*, 4 °C) for serum collection. The sera were stored at − 80 °C before use. The liver was promptly removed and weighed. The same left lobe of the liver tissue was immediately fixed with 10% neutral buffered formalin for 24 h at room temperature and embedded in paraffin for pathological examination. The remaining liver tissues were stored at − 80 °C prior to the RNA and protein assays.

Preliminary mouse experiments

Six BALB/c mice were used for the preliminary experiments. Four of the mice were injected with 2×10^6 $GRA15_{II}$-RAW264.7 cells through the tail vein and the other two were injected with PBS as the control. One $GRA15_{II}$-RAW264.7 cell-infused mouse was euthanized at 24 h, 48 h, 72 h and 7 days. The mouse liver tissues were used to generate frozen sections at the first three time points and for the assessment of Flag protein expression from the $GRA15_{II}$-RAW264.7 cells by western blotting at the last time point.

Western blotting

Four groups of RAW264.7 cells were co-cultured for 72 h with the JS1 cells. The JS1 cells and 100 mg of mouse liver tissues were lysed in ice-cold radio-immunoprecipitation assay buffer supplemented with protease inhibitors and phenylmethanesulfonyl fluoride, and the total protein concentrations were measured using the BCA Protein Assay Kit. Proteins were quantitatively separated through standard SDS-polyacrylamide gel electrophoresis, electrotransferred onto nitrocellulose membranes, probed with the corresponding antibodies, incubated with a horseradish peroxide-conjugated secondary antibody and detected using an ECL kit (Thermo Scientific Inc., Waltham, MA, USA).

The four groups of RAW264.7 cells were collected to detect the expression of the Flag tag (1:1000), iNOS (1:1000), Arg-1 (1:500) and MMP13 (1:800). JS1 cells co-cultured with the above RAW264.7 cells for 72 h were analyzed for α-SMA (1:2000), Col I (1:800) and TGF-β1 (1:1000) expression. Total proteins from mouse liver tissues were subsequently probed with the Flag tag antibody (1:1000). The mouse housekeeping gene encoding GAPDH (1:2000) was used as an internal control to normalize the expression of the target proteins.

RNA extraction and qRT-PCR

Total RNA was extracted from the cultured cells or liver tissues using TRIzol reagent (Invitrogen Life Technologies, Carlsbad, CA, USA) and transcribed into cDNA following the manufacturer's instruction. SYBR Premix Ex Taq (Vazyme, Nanjing, China) was used for cDNA amplification, and quantitative RT-PCR was performed with the ABI Prism 7500 sequence detection system (Applied Biosystems, Foster City, CA, USA). The thermal cycling condition was programmed according to the manufacturer's instructions. GAPDH was used for normalization and as a control for the relative quantitative evaluation of the transcript abundance. Gene expression values from the qRT-PCR were analyzed using the threshold cycle ($2^{-\Delta\Delta Ct}$) method.[36] All qRT-PCR reactions were performed in technical triplicates. The sense and antisense primers are listed in Table 1.

Spleen lymphocyte isolation and cultivation

Spleens were removed aseptically from experimental mice and ground in Hank's medium. The cells were sieved through 75 μm cell filters and lysed with Red Blood Cell Lysis buffer. After washing twice, spleen lymphocytes were adjusted to 2×10^6 cells and seeded into 6-well plates in 1 ml of RPMI 1640 medium supplemented with 10% FBS. The cells were cultured for 6 h while being stimulated with 0.03 μg/ml phorbol 12-myristate 13-acetate and 1 μg/ml ionomycin. The lymphocytes and supernatants were collected separately for qRT-PCR and ELISA.

ELISA

Accurately weighed liver tissues were homogenized with ice-cold PBS (pH 7.4, 10% w/v, 1 g tissue in 10 ml of ice-cold PBS). The homogenates were centrifuged at 12 000*g* for 10 min at 4 °C and small aliquots (0.5 ml) of the resultant supernatants were placed in eppendorf tubes to measure the α-SMA, iNOS, Arg-1, MMP13 and Col I levels (USCN Business Co., Wuhan, China) in the liver tissues by ELISA. The plasma HA level was also quantified using an ELISA kit.

The four groups of RAW264.7 cells (2×10^6 cells) were seeded separately onto 6-well tissue culture plates for 48 h. Supernatants were harvested and assayed for cytokine production (TNF-α, IL-6, IL-10 and TGF-β1). Splenocyte supernatants were assayed for Th1/Th2 cytokine production (IFN-γ, TNF-α, IL-4 and IL-13).

All samples were processed in duplicate according to the manufacturer's guidelines. The absorbance was measured at 450 nm on an ELISA plate reader (Biotek, Winooski, VT, USA).

Table 1 The primers used for qRT-PCR

Primer	*Sense*	*Antisense*
IFN-γ	GGTCAACAACCCACAGGTCC	CGACTCCTTTTCCGCTTCC
IL-4	TCTCGAATGTACCAGGAGCCATATC	AGCACCTTGGAAGCCCTACAGA
IL-10	GCTCCTAGAGCTGCGGACT	TGTTGTCCAGCTGGTCCTTT
TGF-β1	CTGGATACCAACTACTGCTTCAG	TTGGTTGTAGAGGGCAAGGACCT
TNF-α	ACGGCATGGATCTCAAAGAC	GTGGGTGAGGAGCACGTAGT
IL-6	CCGGAGAGGAGACTTCACAG	CATTTCCACGATTTCCCAGA
IL12p40	GATGTCACCTGCCCAACTG	TGGTTTGATGATGTCCCTGA
IL-13	CTTGCTTGCCTTGGTGGTCT	GCACAGGGGAGTCTGGTCTT
α-SMA	GGGAGCAGAACAGAGGAATG	CCAAACAAGGAGCAAAGACG
iNOS	CACCTTGGAGTTCACCCAGT	ACCACTCGTACTTGGGATGC
Col I	GCTCCTCTTAGGGGCCACT	CCACGTCTCACCATTGGGG
MMP13	ACTTAACTTACAGGATTGTGA	GTGCCATCATAGATTCTGGTG
Arg-1	CTCCAAGCCAAAGTCCTTAGAG	AGGAGCTATCATTAGGGACATC
GAPDH	CAACTTTGGCATTGTGGAAGG	ACACATTGGGGGTAGGAACAC

Abbreviations: Arg-1, arginase-1; Col I, type 1 collagen; GAPDH, glyceraldehyde-3-phosphate dehydrogenase; IFN, interferon; IL, interleukin; iNOS, inducible nitric synthase; MMP13, matrix metalloproteinase 13; α-SMA, α-smooth muscle actin; TNF, tumor necrosis factor;TGF-β1, transforming growth factor beta 1.

Arginase activity assay and nitrite analysis

The four groups of RAW264.7 cells (2×10^6) were cultured for 48 h, and the supernatants were measured for NO and arginase activity. The nitrite content was a reflection of the NO production and was determined using the Griess Reagent System (Promega Biotech Co., Madison, WI, USA) as previously described[37] and expressed as a millimolar concentration according to the manufacturer's instruction. The arginase activity was measured using a colorimetric method as previously described,[38] and the urea accumulation was quantified. Briefly, 10 mM $MnCl_2$ and 0.5 ml of arginine were successively added to the supernatants for 1 h at 37 °C. The reaction was stopped by the addition of an acidic solution (H_2SO_4:H_3PO_4:H_2O = 1:3:7). The optical densities (ODs) of both solutions were measured at 550 nm on an ELISA plate reader (Biotek).

Hepatic hydroxyproline

The hepatic hydroxyproline (Hyp) content was used as an indirect measure of tissue collagen.[39] The Hyp concentration in liver tissues (100 mg) was determined with a commercially available kit (Jiancheng Biological Engineering Research Institute, Nanjing, China). The Hyp content is expressed as μg/mg of liver wet weight.

Histology and IHC of liver sections

The liver specimens were embedded in paraffin blocks and cut into 4-mm-thick sections to examine the size of the granuloma by HE staining. Masson staining was used to detect the extent of hepatic fibrosis according to the manufacturer's instructions. The same portion of hepatic tissues was weighed accurately and digested in 5% sodium hydroxide (NaOH) solution at 65 °C for 1 h to count schistosome eggs. The results are expressed as the number of eggs per gram of liver. IHC of the hepatic granuloma was conducted as previously described.[40] Immunostaining for α-SMA (1:1000), Col I (1:250), TGF-β1 (1:300) and MMP13 (1:150) was performed. The samples were incubated overnight at 4 °C with primary antibodies and then with biotinylated secondary antibodies for 45 min. Quantitative and qualitative changes were analyzed using morphometric software (Image-Pro Plus software, Media Cybernetics, Inc., Rockville, MD, USA).

Statistical analysis

The statistical analysis of the animal experiments was performed with samples from 5 mice, and the analysis of the cell experiments was performed with four biological replicates. Quantitative data are expressed as the mean ± s.d. The experimental data obtained were subjected to statistical analysis using one-way ANOVA followed by Tukey's multiple comparison test for comparison between the treatment and LV-RAW264.7 group. Correlations were determined using Pearson's test. All statistical analyses were performed using GraphPad Prism Version 5.00 (GraphPad Software, San Diego, CA, USA). Differences were considered statistically significant for *P*-values <0.05.

RESULTS

Transfected macrophages expressed $GRA15_{II}$ or $ROP16_{I/III}$

The cells were observed under the fluorescence microscope to verify the transfection of the recombinant lentivirus plasmids. A large number of green fluorescent cells were observed, indicating the successful transfection and GFP expression in the RAW264.7 cells (Figure 1a). The transfected RAW264.7 cells were selected with PM due to the presence of an anti-PM gene site in the lentivirus. Different PM concentrations were added to the medium of the treated RAW264.7 cells in 96-well cell culture plates to generate a gradient. The efficiency of $GRA15_{II}$-RAW264.7, $ROP16_{I/III}$-RAW264.7 and LV-RAW264.7

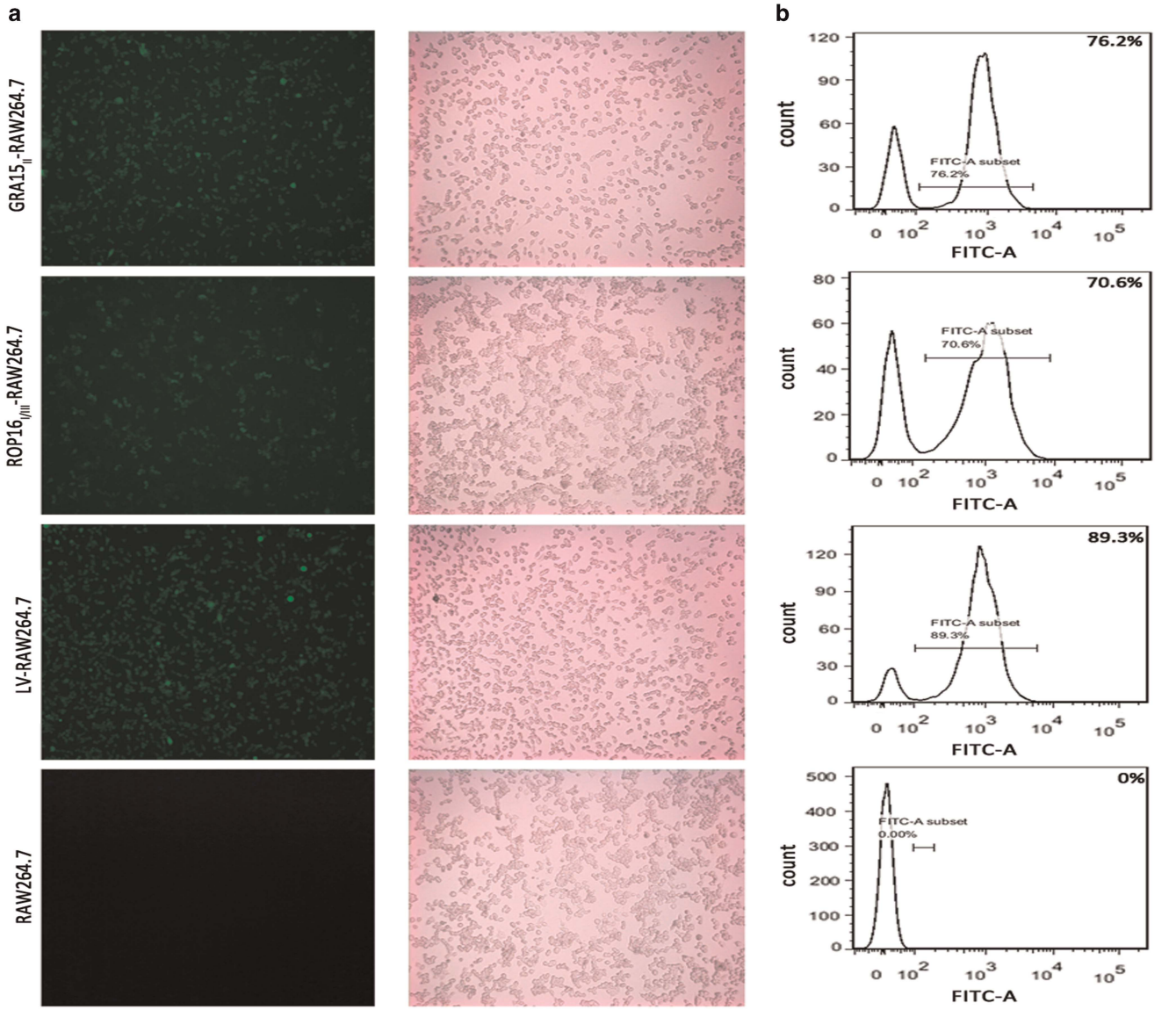

Figure 1 RAW264.7 cells were transfected with *gra15*$_{II}$ or *rop16*$_{I/III}$ fused to pEGFP. (**a**) $GRA15_{II}$ or $ROP16_{I/III}$ expression was examined through green fluorescent protein expression using fluorescence microscopy. (**b**) The cell transfection efficiency was determined by flow cytometry.

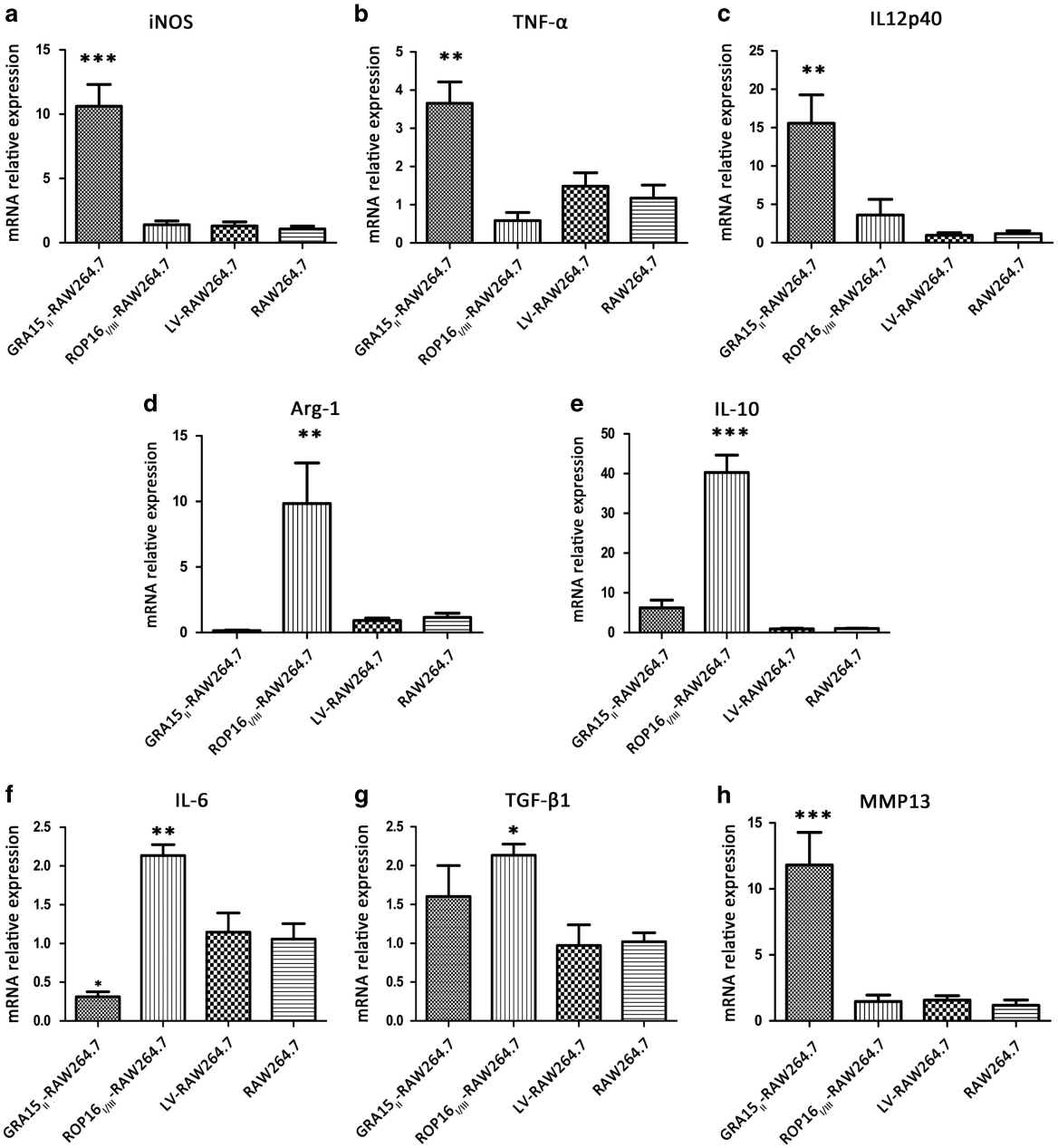

Figure 2 The relative mRNA expression of iconic proteins and cytokines in transfected RAW264.7 and control RAW264.7 cells was examined by qRT-PCR following normalization with GAPDH. The mRNA expression levels of iNOS (**a**), TNF-α (**b**), IL12p40 (**c**), and MMP13 (**h**) increased sharply and IL-6 (**f**) was downregulated in $GRA15_{II}$-RAW264.7 cells. The relative mRNA expression levels of Arg-1 (**d**), IL-10 (**e**), IL-6 (**f**) and TGF-β1 (**g**) were increased in the $ROP16_{I/III}$-RAW264.7 control cells compared to the LV-RAW264.7 cells. No significant difference in the index was found between the LV-RAW264.7 and RAW264.7 cells (*$P<0.05$, **$P<0.01$, ***$P<0.001$, $n=4$). Arg-1, arginase-1; GAPDH, glyceraldehyde-3-phosphate dehydrogenase; iNOS, inducible nitric synthase; IL, interleukin; MMP13, matrix metalloproteinase 13; mRNA, messenger RNA; qRT-PCR, quantitative real-time PCR; TNF, tumor necrosis factor.

construction was 76.2%, 70.6% and 89.3% when PM was used at concentrations of 5, 2.2 and 6 μg/ml, respectively (Figure 1b).

$GRA15_{II}$ promoted macrophages to adopt an M1-like phenotype and $ROP16_{I/III}$ induced an M2-like cell bias

We evaluated the polarization of macrophages with stable $GRA15_{II}$ or $ROP16_{I/III}$ expression. The relative mRNA expression analysis of treated RAW264.7 cells by qRT-PCR (Figure 2) showed that iNOS ($P<0.001$), TNF-α ($P<0.05$) and IL12p40 ($P<0.01$) were remarkably increased but IL-6 ($P<0.05$) was decreased in the $GRA15_{II}$-RAW264.7 cells compared with the LV-RAW264.7 cells. In contrast, the Arg-1 ($P<0.05$), IL-10 ($P<0.001$), IL-6 ($P<0.01$) and TGF-β1 ($P<0.05$) mRNA levels were upregulated in the $ROP16_{I/III}$-RAW264.7 control cells compared with the LV-RAW264.7 cells. No significant

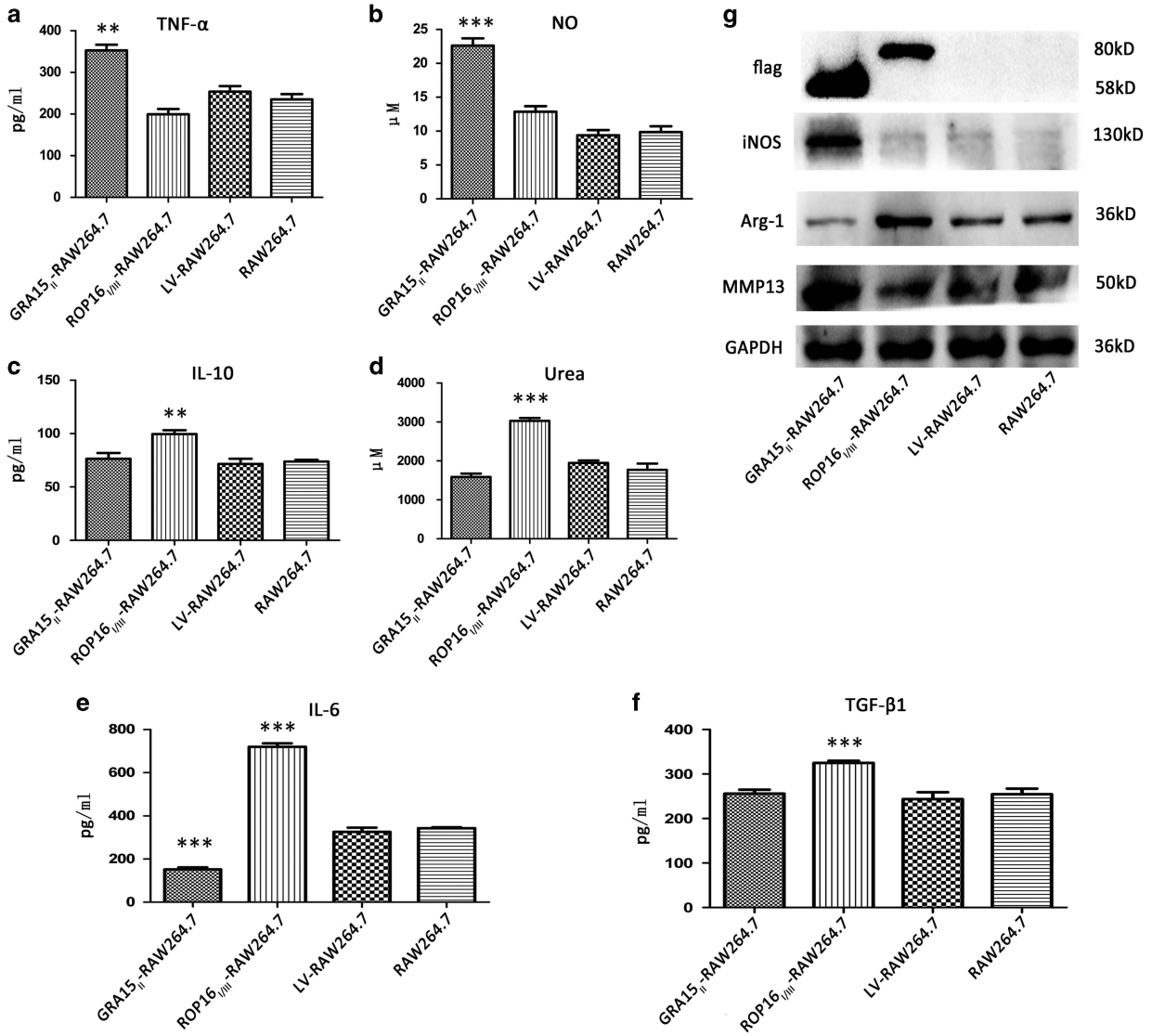

Figure 3 Cytokine expression was altered in the RAW264.7 cells by transfection of the target genes (*gra15*$_{II}$ or *rop16*$_{I/III}$). The culture supernatants were collected and analyzed for TNF-α (**a**), NO (**b**), IL-10 (**c**), urea (**d**), IL-6 (**e**) and TGF-β1 (**f**) production by the transfected RAW264.7 and control RAW264.7 cells. The TNF-α and NO levels were enhanced and IL-6 was decreased in the GRA15$_{II}$-RAW264.7 cells, whereas the IL-10, urea, IL-6 and TGF-β1 levels were increased in the ROP16$_{I/III}$-RAW264.7 control cells compared with the LV-RAW264.7 cells. The transfected macrophage-related proteins Flag, iNOS, Arg-1 and MMP13 were detected by western blotting (**g**). The Flag tag was expressed with an approximate molecular weight of 58 kD (GRA15$_{II}$-RAW264.7 cells) and 80 kD (ROP16$_{I/III}$-RAW264.7 cells). Higher iNOS and MMP13 expression levels were detected in the GRA15$_{II}$-RAW264.7 cells compared with the LV-RAW264.7 cells. Correspondingly, escalated Arg-1 expression was detected in the ROP16$_{I/III}$-RAW264.7 cells compared to the LV-RAW264.7 cells (**$P<0.01$, ***$P<0.001$, $n=4$). Arg-1, arginase-1; IL, interleukin; iNOS, inducible nitric synthase; MMP13, matrix metalloproteinase 13; NO, nitric oxide; TNF, tumor necrosis factor; TGF-β1, transforming growth factor beta 1.

difference was detected in TGF-β1 expression between the GRA15$_{II}$-RAW264.7 and LV-RAW264.7 cells. The secretion of inflammatory factors into the cell supernatants was determined by ELISA (Figure 3). The results in agreement with the relative mRNA expression levels were confirmed with the exception of IL12p40, which was expressed at an obviously low level (data not shown). Additionally, the NO concentration ($P<0.001$) was markedly increased in the GRA15$_{II}$-RAW264.7 cells (Figure 3b) and urea production ($P<0.001$) was noticeably increased in the ROP16$_{I/III}$-RAW264.7 control cells (Figure 3d) compared with the LV-RAW264.7 cells. iNOS and Arg-1 protein expression determined by western blotting coincided with the mRNA transcript levels. The relative mRNA transcript (Figure 2h) and protein expression levels of MMP13 (Figure 3g) were significantly enhanced in the GRA15$_{II}$-RAW264.7 cells but not in the ROP16$_{I/III}$-RAW264.7 control cells compared with the LV-RAW264.7 cells. Additionally, Flag tag expression was confirmed by western blotting. As expected,

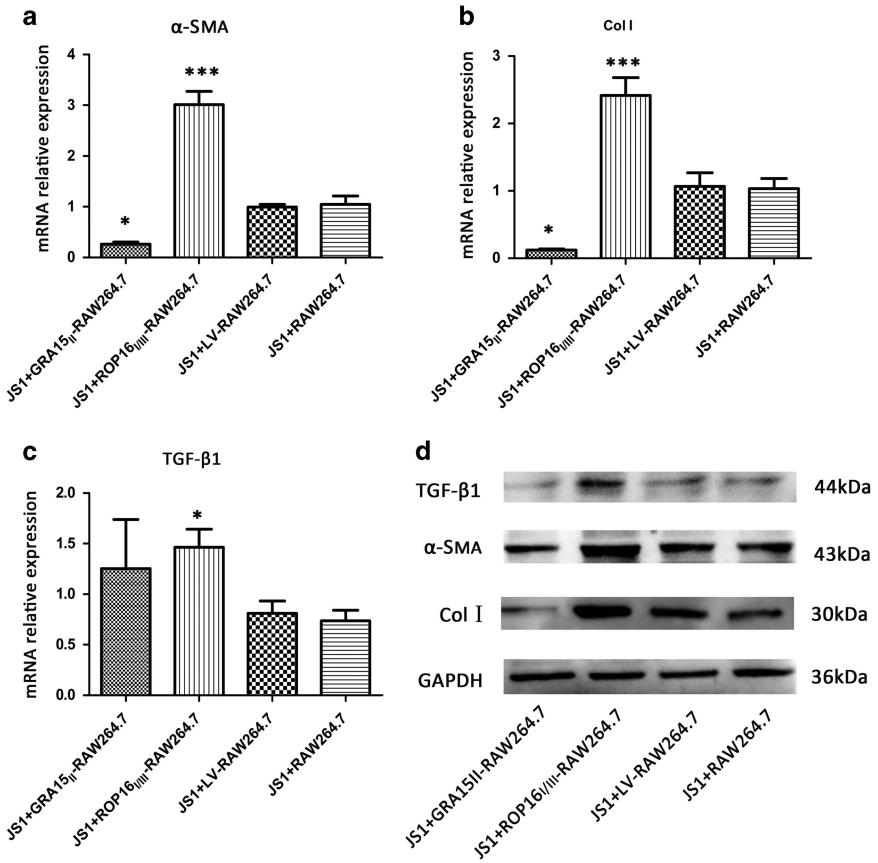

Figure 4 $GRA15_{II}$-polarized RAW264.7 cells exhibited decreased expression of the profibrogenic factor profile *in vitro*. $GRA15_{II}$-RAW264.7 weakened JS1 fibrogenic activities and $ROP16_{I/III}$-RAW264.7 control cells promoted the activities based on the measurement of mRNA (**a**–**c**) and protein (**d**) relative expression levels of α-SMA, Col I and TGF-β1 in the JS1 cells after co-culturing. No significant difference was detected between JS1 cells co-cultured with LV-RAW264.7 and RAW264.7 cells. JS1 cells produced a decreased level of α-SMA and Col I when co-cultured with $GRA15_{II}$-RAW264.7 cells and an enhanced level when co-cultured with $ROP16_{I/III}$-RAW264.7 cells compared with the LV-RAW264.7 control cells. Simultaneously, escalated TGF-β1 expression was noted in the $ROP16_{I/III}$-RAW264.7 group ($^*P<0.05$, $^{***}P<0.001$, $n=4$). Col I, type 1 collagen; α-SMA, α-smooth muscle actin; TGF-β1, transforming growth factor beta 1.

$GRA15_{II}$ and $ROP16_{I/III}$ had approximate molecular weights of 58 and 80 kD, respectively (Figure 3g).

$GRA15_{II}$-RAW264.7 cells had decreased profibrogenic factor profile expression *in vitro*

The fibrosis-related indices of JS1 cells, including α-SMA, Col I and TGF-β1, were analyzed by qRT-PCR and western blotting. No difference was found between JS1 cells co-cultured with LV-RAW264.7 and RAW264.7 cells. The relative α-SMA ($P<0.05$) and Col I ($P<0.05$) mRNA expression levels in the JS1 cells were downregulated in the $GRA15_{II}$-RAW264.7 co-cultured group but increased in the $ROP16_{I/III}$-RAW264.7 co-cultured group ($P<0.001$) compared with the LV-RAW264.7 cells (Figures 4a and b). Moreover, TGF-β1 mRNA expression ($P<0.05$) was elevated in the $ROP16_{I/III}$-RAW264.7 co-cultured JS1 cells but no significant difference in expression was found in the $GRA15_{II}$-RAW264.7 cell coculture ($P>0.05$; Figure 4c). Parallel results were confirmed by western blotting (Figure 4d).

$GRA15_{II}$-RAW264.7 cells attenuated hepatic fibrosis by suppressing α-SMA, Col I and TGF-β1 expression

Observation of frozen mouse liver tissue sections under the fluorescence microscope revealed that the $GRA15_{II}$-RAW264.7 cells were alive (Figure 5a). The Flag protein was detectable in the mouse liver tissues by western blotting 7 days after the cell transfer (Figure 5b), indicating the relatively long survival of the inoculated cells in the mouse liver after tail vein administration.

The mice were inoculated with the cells and then infected with schistosome cercariae in combination with a second dose of the cells 7 days later. Experimental mice were killed under euthanasia 56 days post infection with the schistosomes. The gross liver specimens from the $GRA15_{II}$-RAW264.7-treated animals showed a fleshy pink color, fewer granulomas (Figure 5c) and remarkably reduced egg counts (Figure 5c1) compared with the other groups of mice. HE staining (Figure 5d) and Masson staining (Figure 5e) exhibited obviously alleviated liver pathological lesions in the $GRA15_{II}$-RAW264.7 cell-treated mice compared with the LV-RAW264.7

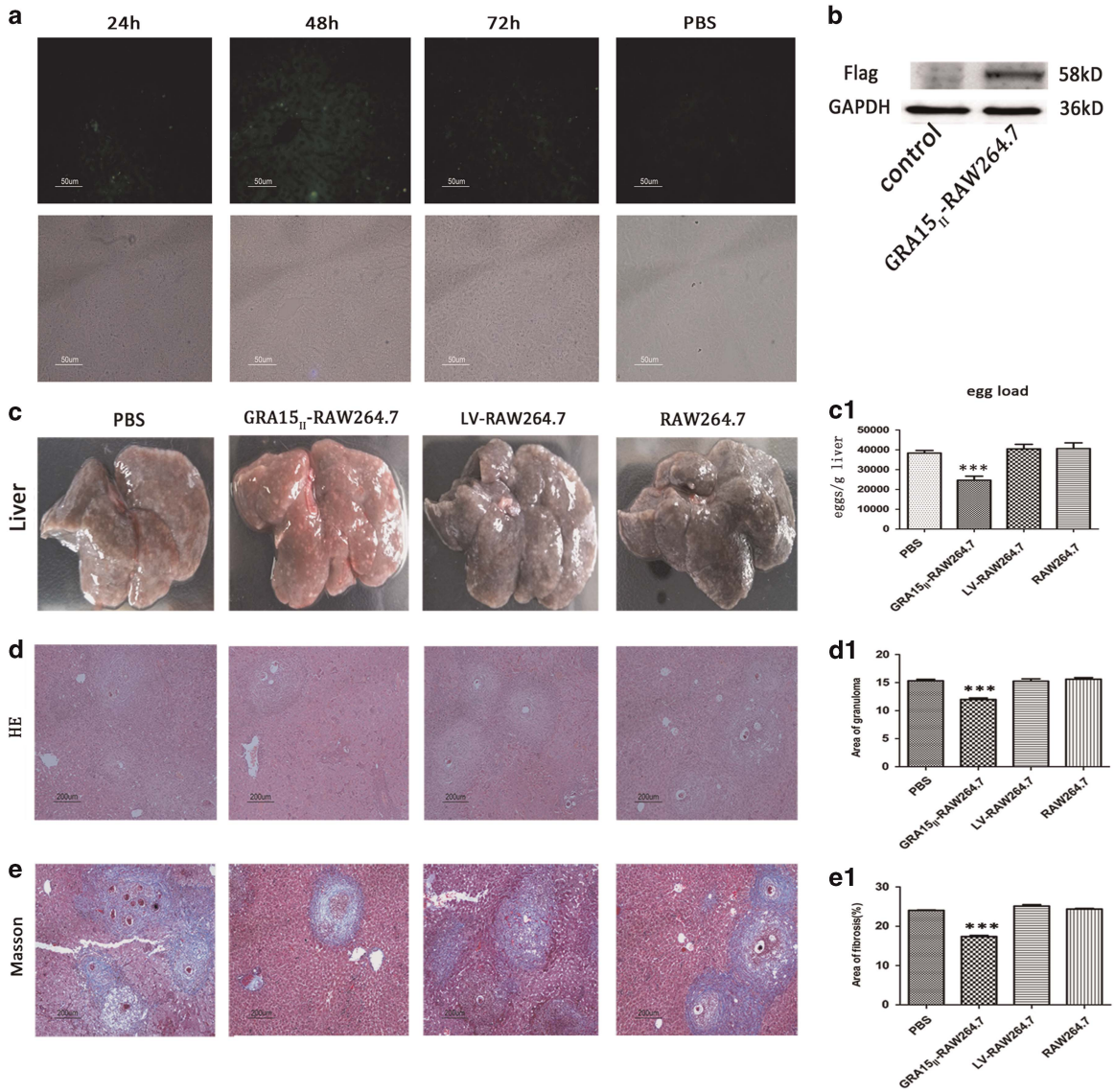

Figure 5 $GRA15_{II}$-RAW264.7 reached the liver tissues and survived. (**a**) Mouse liver frozen sections were observed under the fluorescence microscope. Samples were collected at 24, 48 and 72 h after $GRA15_{II}$-RAW264.7 cell transfer. (**b**) The Flag tag was detected in mouse liver tissues 7 days after $GRA15_{II}$-RAW264.7 cell transfer by western blotting. Pre-injection of $GRA15_{II}$-RAW264.7 cells diminished liver pathological lesions in schistosome-infected mice. The livers were removed and shown in **c**. The egg load was lower in the $GRA15_{II}$-RAW264.7-treated mice compared with the LV-RAW264.7-treated mice (**c1**). HE staining to show the granuloma area (**d**) and data analysis (**d1**). Masson staining was performed to assess the extent of hepatic fibrosis (**e**); the statistical analysis is shown in (**e1**). No significant difference in the pathological lesion index was observed between the LV-RAW264.7, RAW264.7 and PBS control mice. All asterisks indicate significant differences between the $GRA15_{II}$-RAW264.7 and LV-RAW264.7-treated mice (***$P<0.001$, $n=5$). HE, hematoxylin and eosin; PBS, phophate-bufferred saline.

cell-treated mice ($P<0.001$; Figures 5d1 and e1). No pathological change was evident in the LV-RAW264.7, RAW264.7 and PBS control animals. Fibrosis-inducing factors such as α-SMA, Col I, MMP13 and TGF-β1 were detected in the liver tissues by IHC (Figures 6a–d), qRT-PCR (Figures 7a–d) and ELISA (Figures 8a–c). Correspondingly, the serum HA levels ($P<0.001$; Figure 8f) and liver Hyp content ($P<0.001$; Figure 8g) were significantly decreased in the $GRA15_{II}$-RAW264.7 cell-transferred mice.

$GRA15_{II}$-skewed macrophages enhanced liver MMP13 expression and promoted the host Th1 response

Mice were administered $GRA15_{II}$-RAW264.7 cells followed by schistosome infection. Consequently, all animals exhibited notable increases in mRNA transcription of MMP13 ($P<0.01$; Figure 7d) and iNOS ($P<0.05$; Figure 7e) together with elevated IFN-γ ($P<0.01$) and TNF-α ($P<0.05$) mRNA expression (Figure 9a). No change was observed in the Arg-1 mRNA level ($P>0.05$; Figure 7f). In contrast, mice injected

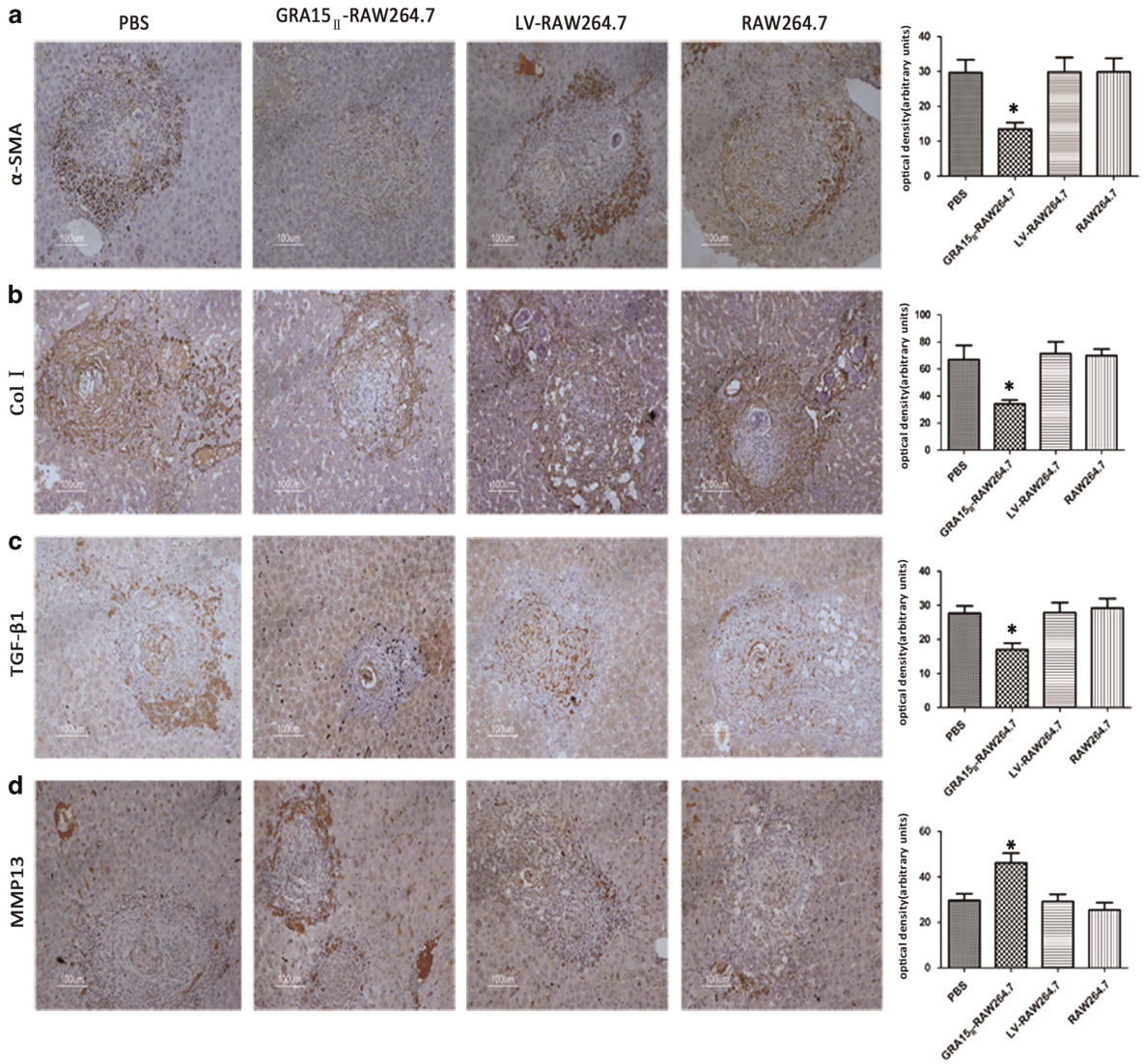

Figure 6 Pre-injection of GRA15$_{II}$-RAW264.7 cells suppressed liver fibrosis in schistosome-infected mice based on the protein expression levels of α-SMA (**a**), Col I (**b**) and TGF-β1 (**c**) and the upregulation of MMP13 expression (**d**) analyzed by IHC compared with infection of LV-RAW264.7 cells. No difference was found among the LV-RAW264.7, RAW264.7 and PBS groups (*$P<0.05$, $n=5$). Col I, type 1 collagen; IHC, immunohistochemistry; MMP13, matrix metalloproteinase 13; α-SMA, α-smooth muscle actin; TGF-β1, transforming growth factor beta 1.

with GRA15$_{II}$-RAW264.7 cells presented a dramatic reduction in the IL-4 ($P<0.001$) and IL-13 mRNA levels ($P<0.01$) compared with the LV-RAW264.7 group (Figure 9a).

Parallel MMP13, iNOS and Arg-1 expression results were obtained by ELISA in the liver homogenate supernatants (Figure 8c-e). Additionally, similar levels of the cytokines IFN-γ, TNF-α, IL-4 and IL-13 were detected in the pooled mouse serum and spleen lymphocyte supernatant samples (Figure 9b).

DISCUSSION

The key pathogenesis of *S. japonica* includes granuloma formation due to the deposition of parasite eggs in the liver. A granuloma consists of infiltrated lymphocytes, macrophages (Kupffer cells), eosinophils, neutrophils and collagen fibers that surround mature eggs containing larvae that produce soluble egg antigens. Granuloma development possibly results in hepatic fibrosis followed by cirrhosis, which continues to be a significant cause of death[41] although the entrapment of the eggs by inflammation is considered a self-protective process.

In the murine model, mice deficient in the type 1 cytokines IFN-γ and IL12p40 showed little alteration in pathology. In contrast mice deficient in type 2 cytokines were unable to generate a granuloma.[42] Thus, hepatic fibrosis was reported to be caused by gene transcription pathways associated with collagen synthesis and matrix remodeling promoted by type 2-mediated cytokines, such as IL-4 and IL-13.[43] Additionally,

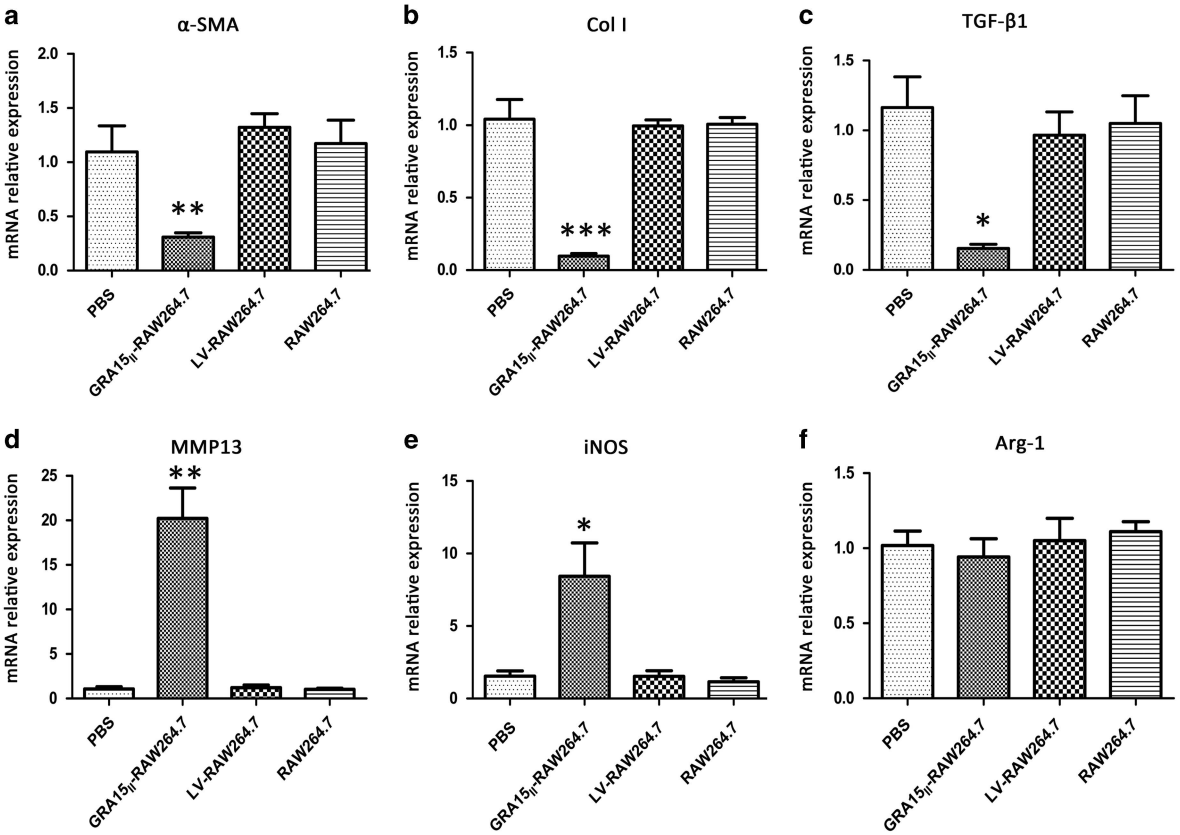

Figure 7 The relative mRNA expression levels of fibrosis-related genes were examined in the liver tissues of schistosome-infected mice by qRT-PCR. The mRNA expression levels of α-SMA (**a**), Col I (**b**) and TGF-β1 (**c**) were significantly reduced and MMP13 (**d**) and iNOS (**e**) were elevated in the $GRA15_{II}$-RAW264.7 mice but not difference was observed in Arg-1 (**f**) (*$P<0.05$, **$P<0.01$, ***$P<0.001$, $n=5$). Arg-1, arginase-1; Col I, type 1 collagen; iNOS, inducible nitric synthase; mRNA, messenger RNA; MMP13, matrix metalloproteinase 13; qRT-PCR, quantitative real-time PCR; α-SMA, α-smooth muscle actin; TGF-β1, transforming growth factor beta 1.

TGF-β1 has been proposed to be a critical factor for the activation of the "resting" hepatic stellate cells (HSCs) responsible for hepatic fibrogenesis.[44–46]

Macrophages have a pivotal role in granuloma formation and the development of hepatic fibrosis during schistosomiasis.[4,8,47] Classically activated macrophages (M1 cells) mediate resistance to intracellular pathogens through the expression of cytokines and chemokines such as IL-12, CXCL9 and CXCL10, which promote the Th1 dominant response.[48–50] In contrast, alternatively activated macrophages (M2 cells) are critically involved in granuloma formation and fibrosis via the Th2 cytokine response.[19,43,51–54]

Recent studies revealed that the polymorphic dense granule protein $GRA15_{II}$ and rhoptry protein $ROP16_{I/III}$ secreted by type II or type I/III *Toxoplasma* induced differential macrophage polarization.[36,46] $GRA15_{II}$, which is a protein with no homology to other proteins, actively evokes the responsiveness of infected host cells via the NF-κB signaling pathway and induces macrophages towards an M1 cell phenotype, whereas $ROP16_{I/III}$, which is an active kinase that directly phosphorylates the STAT6/STAT3 transcription factors, induces macrophages to resemble aspects of M2 cells.[27,33,46]

Our previous work revealed that *T. gondii* genotype Chinese 1 predominantly circulated in animals and humans in China and contained a $GRA15_{II}$ that was identical to the type II strains and a $ROP16_{I/III}$ homologous to the type I strains. The $ROP16_{I/III}$ allele has a leucine (L) at position 503 similar to the RH strain, which is responsible for the induction of M2 cell polarization.[55] Therefore, we established a novel strategy to directionally drive M1 cell polarization *in vivo* using $GRA15_{II}$ to explore the inhibitory effect on the hepatic granuloma formation and fibrosis processes. The *in vitro* experiments indicated that the $gra15_{II}$-transfected RAW264.7 macrophages presented M1-like cell phenotypes based on the high iNOS, TNF-α and IL12p40 transcription, high iNOS and TNF-α protein expression levels and elevated nitric oxide production that coincided with the reported M1 iconic indicators[56,57] with the exception of the IL12p40 protein level. In contrast, the $rop16_{I/III}$-transfected macrophages showed a distinctive index of Arg-1, IL-10, and TGF-β1 expression that was consistent with the reported M2 phenotype[6,46,56–58] with the exception of IL-6. Moreover, IL12p40 is linked to NF-κB activation and is highly expressed in type 2 *Toxoplasma*-infected macrophages *in vitro*.[31,59] In the present experiments, no significant

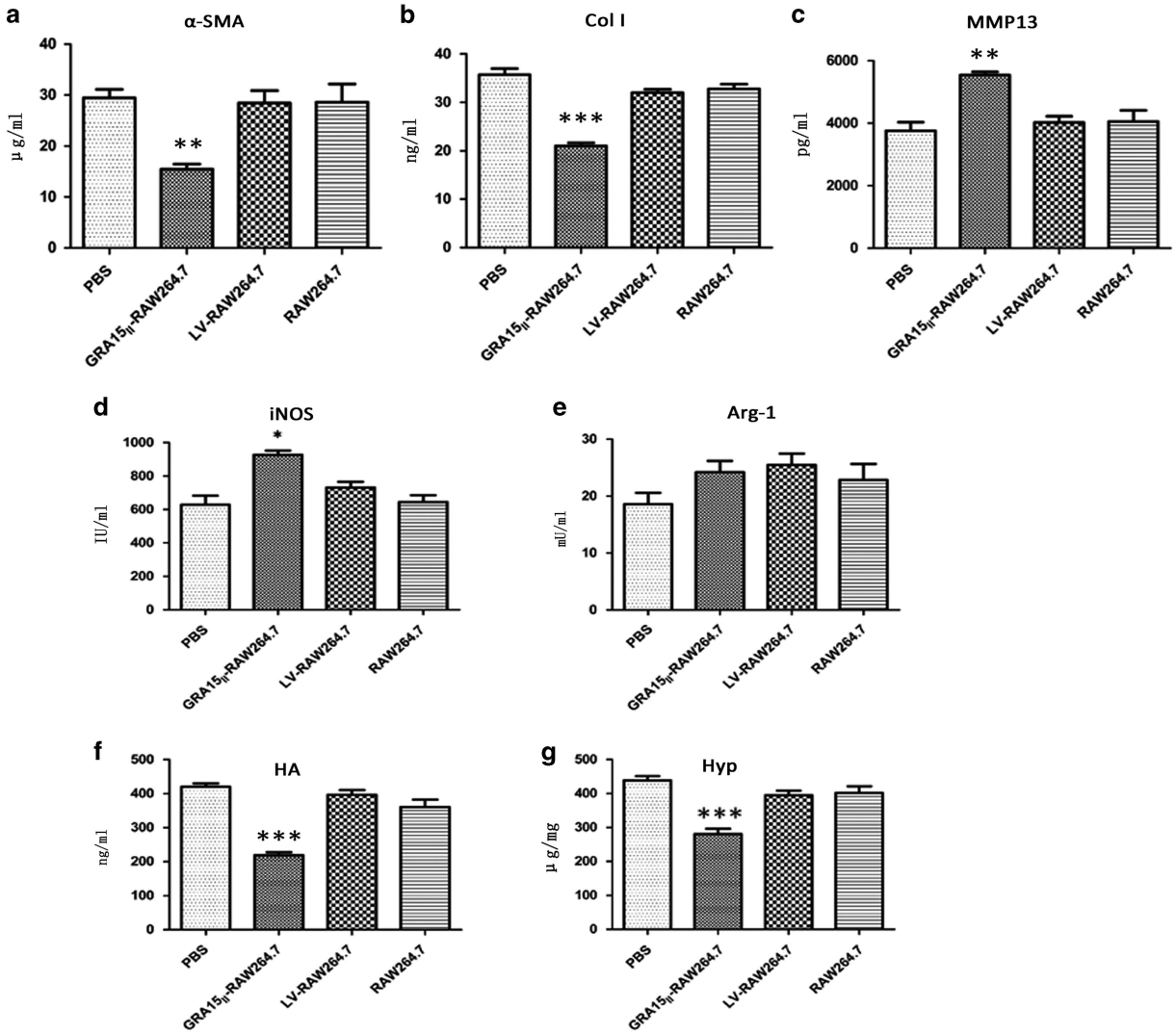

Figure 8 Liver fibrosis-related proteins in the liver homogenate supernatants from schistosome-infected mice were tested by ELISA (**a**–**e**). The α-SMA and Col I levels were decreased and the MMP13 and iNOS were enhanced but no difference was detected in Arg-1 in the $GRA15_{II}$-RAW264.7-treated mice. HA was also quantified in the serum samples using an ELISA kit (**f**), and the Hyp content was determined by alkaline hydrolysis in the liver tissues (**g**). Lower HA and Hyp expression levels were detected in mice treated with $GRA15_{II}$-RAW264.7 cells than in mice treated with LV-RAW264.7 cells (*$P<0.05$, **$P<0.01$, ***$P<0.001$, $n=5$). Arg-1, arginase-1; Col I, type 1 collagen; ELISA, enzyme-linked immunosorbent assay; HA, hyaluronic acid; Hyp, hydroxyproline; iNOS, inducible nitric synthase; MMP13, matrix metalloproteinase 13.

difference in IL12p40 protein expression was found between the $GRA15_{II}$-RAW264.7 cells and LV-RAW264.7 control cells. In contrast to the previous report,[55] IL-6 expression was decreased in the $GRA15_{II}$-RAW264.7 cells and significantly upregulated in the $ROP16_{I/III}$-RAW264.7 cells. The reason for the discrepancy is unknown.

Furthermore, the $GRA15_{II}$-RAW264.7 cells had the capacity to mediate the restraint of fibrogenesis-related proteins by the murine hepatic stellate JS1 cell line, whereas $ROP16_{I/III}$-RAW264.7 cells promoted fibrogenesis via up-modulating α-SMA, Col I and TGF-β1 production in the JS1 cells in a co-culture system. This result was similar to the result obtained in a previous investigation that indicated that M1 cells inhibited co-cultured myofibroblast complex matrix deposition.[7,60] Our data strongly suggested that the Apicomplexan *Toxoplasma*-derived protein $GRA15_{II}$ but not the viable parasite might efficiently drive macrophage polarization towards M1 cells, which coincided with the previous reports by Jensen *et al.*[33] and Murray[55] *Tg*$GRA15_{II}$ is one of the polymorphic effectors secreted from *Toxoplasma* dense granules and may activate NF-κB and drive the pro-inflammatory M1 gene expression program during the early phase of *Toxoplasma* infection that constitutes the host innate immune response against the parasite.

We found high generation of TNF-α in the $GRA15_{II}$-RAW264.7 cells and increased TGF-β1 production in the $ROP16_{I/III}$-RAW264.7 cells. TNF-α has a negative effect on p38 MAPK phosphorylation and is an anti-apoptotic and

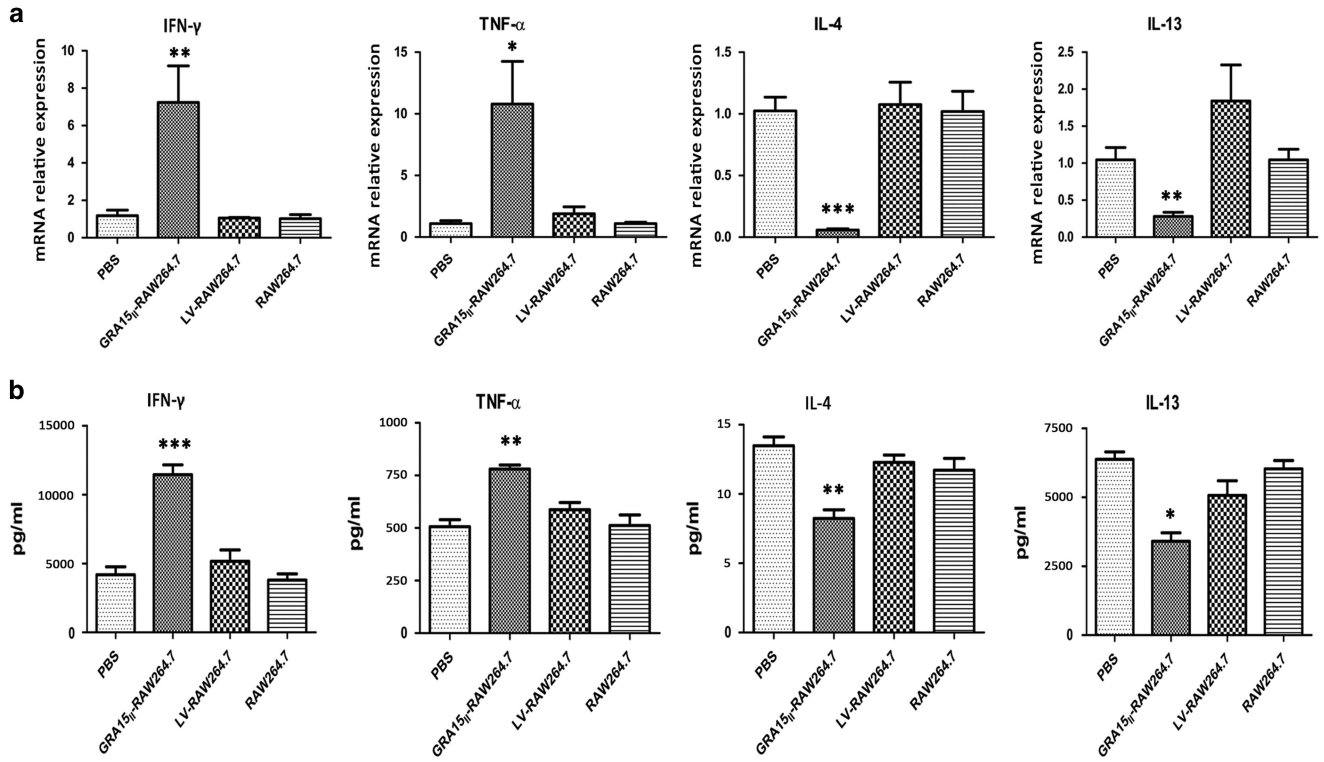

Figure 9 Pre-transfer of $GRA15_{II}$-RAW264.7 cells evoked Th1-associated immunity to schistosome infection. (**a**) The relative mRNA expression levels of Th1 cytokines (IFN-γ and TNF-α) were increased and Th2 cytokines (IL-4 and IL-13) were reduced in spleen lymphocytes from $GRA15_{II}$-RAW264.7 mice. Parallel results were noted by ELISA in the pooled mouse serum and spleen lymphocyte supernatant samples (**b**). No significant difference was observed among mice injected with PBS, RAW264.7 cells and LV-RAW264.7 cells ($^*P<0.05$, $^{**}P<0.01$, $^{***}P<0.001$, $n=5$). ELISA, enzyme-linked immunosorbent assay; IFN, interferon; IL, interleukin; PBS, phosphate-buffered saline; TNF, tumor necrosis factor.

anti-proliferative factor for HSCs, whereas TGF-β1 is a powerful profibrogenic cytokine and has a key role in HSC activation and proliferation.[61] Additionally, high expression of MMP13 was observed in the $GRA15_{II}$-RAW264.7 cells, which was reported to contribute to the spontaneous regression of complex extracellular matrices.[62]

The majority of investigations have indicated that M1 cells inhibit proliferation and collagen synthesis in fibroblasts[60] and the liver collagen deposition by which the granulomatous pathology is shaped,[21] resulting in amelioration of the hepatic fibrotic process. Thus, we presumed that $GRA15_{II}$-induced M1 cells might potentially alleviate fibrogenesis, including the liver fibrosis caused by schistosomiasis.

Due to the functional characteristics of the M1 cells induced by *Tg*$GRA15_{II}$, we inoculated mice with the polarized macrophages followed by infection with *S. japonicum*, which induces progressive liver fibrotic lesions associated with the M2/Th2 response. Fibrosis was noticeably alleviated (Figure 5) and the expression of profibrogenic factors such as α-SMA, Col I and TGF-β1 was decreased when $GRA15_{II}$-RAW264.7 cells were administered to mice followed by schistosome cercariae infection. In our previous study, $GRA15_{II}$-RAW264.7 cell transfusion did not have an influencing impact on either the pathology of hepatic tissues or the production of profibrogenic factors when the cells were administered at weeks 3, 4, 5 or 6 after schistosome infection (data not shown), suggesting that smaller granulomas and less collagen deposition might be related to preconditioned Th1 dominant immunity in the liver. Administration of $GRA15_{II}$-activated M1 cells induced a Th1/Th2 re-balance based on the promoted production of IFN-γ, TNF-α, iNOS, and MMP13 and the downregulated expression of IL-4, IL-13 and TGF-β1. As shown in Figures 3b and g, the $GRA15_{II}$-RAW264.7 cells induced high expression of iNOS, which generates NO in *Schistosoma*-infected mice. NO is thought to be cytotoxic to schistosomes and thus may restrain hepatic fibrosis,[6,16,20,63,64] which coincides with the reduced liver egg counts in the $GRA15_{II}$-RAW264.7 cell recipient mice. Studies have also reported that cytokines (TNF-α, IL-12 and INF-γ) and NO are associated with the Th1 response and have an inhibitory impact on fibrosis in schistosomiasis.[19,65] Furthermore, the elevated MMP13 expression in the liver tissues of the $GRA15_{II}$-RAW264.7-treated mice may directly dissolve the extracellular matrix and remodel the fibrotic liver as previously reported.[54]

Taken together, we present evidence for the first time that the $GRA15_{II}$ virulence-associated effector from *T. gondii* may induce M1 phenotype skewing of mouse macrophages and

alter the cytokine profiles that contribute to granulomatous formation and fibrogenesis during the early stage of *S. japonicum* infection, leading to an ameliorative effect on hepatic fibrosis in mice. The present investigation may contribute to the understanding of the mechanism by which M2/Th2 predominant immune responses are involved in the hepatic fibrogenesis caused by schistosomiasis and provide a potential strategy for fibrotic disease involving M1 macrophages driven by the nontoxic peptide derived from the protozoon parasite.

CONFLICT OF INTEREST

The authors declare no conflict of interest.

ACKNOWLEDGEMENTS

We thank Dr Jinsheng Guo at Shanghai Zhongshan Hospital for providing the murine hepatic stellate cell line JS1. The work was funded by the National Science Foundation of China (No. 81471983 and No. 81171606), the National Basic Research Program of China (No. 2010CB530001) and the Science Foundation of Anhui Province (No. KJ2014A106 and No. 1308085MH124).

AUTHOR CONTRIBUTIONS

JS, DC and YX conceived and designed the trial and critically revised the manuscript. YX, HW and KY performed the experiments, performed the statistical analysis and wrote the manuscript. All authors have read and approved the final manuscript.

1 Wilson MS, Mentink-Kane MM, Pesce JT, Ramalingam TR, Thompson R, Wynn TA. Immunopathology of schistosomiasis. *Immunol Cell Biol* 2007; **85**: 148–154.
2 Bergquist R, Utzinger J, McManus DP. Trick or treat: the role of vaccines in integrated schistosomiasis control. *PLoS Negl Trop Dis* 2008; **2**: e244.
3 McManus DP, Loukas A. Current status of vaccines for schistosomiasis. *Clin Microbiol Rev* 2008; **21**: 225–242.
4 Burke ML, Jones MK, Gobert GN, Li YS, Ellis MK, McManus DP. Immunopathogenesis of human schistosomiasis. *Parasite Immunol* 2009; **31**: 163–176.
5 Everts B, Hussaarts L, Driessen NN, Meevissen MH, Schramm G, van der Ham AJ *et al. Schistosome*-derived omega-1 drives Th2 polarization by suppressing protein synthesis following internalization by the mannose receptor. *J Exp Med* 2012; **209**: 1753–1767; S1751.
6 Barron L, Wynn TA. Macrophage activation governs schistosomiasis-induced inflammation and fibrosis. *Eur J Immunol* 2011; **41**: 2509–2514.
7 Duffield JS, Forbes SJ, Constandinou CM, Clay S, Partolina M, Vuthoori S *et al.* Selective depletion of macrophages reveals distinct, opposing roles during liver injury and repair. *J Clin Invest* 2005; **115**: 56–65.
8 Wynn TA, Barron L. Macrophages: master regulators of inflammation and fibrosis. *Semin Liver Dis* 2010; **30**: 245–257.
9 Mosser DM, Edwards JP. Exploring the full spectrum of macrophage activation. *Nat Rev Immunol* 2008; **8**: 958–969.
10 Martinez FO, Helming L, Gordon S. Alternative activation of macrophages: an immunologic functional perspective. *Annu Rev Immunol* 2009; **27**: 451–483.
11 Horsnell WG, Brombacher F. Genes associated with alternatively activated macrophages discretely regulate helminth infection and pathogenesis in experimental mouse models. *Immunobiology* 2010; **215**: 704–708.
12 Gordon S. Alternative activation of macrophages. *Nat Rev Immunol* 2003; **3**: 23–35.
13 Murray PJ, Allen JE, Biswas SK, Fisher EA, Gilroy DW, Goerdt S *et al.* Macrophage activation and polarization: nomenclature and experimental guidelines. *Immunity* 2014; **41**: 14–20.
14 Dewals BG, Marillier RG, Hoving JC, Leeto M, Schwegmann A, Brombacher F. IL-4Ralpha-independent expression of mannose receptor and Ym1 by macrophages depends on their IL-10 responsiveness. *PLoS Negl Trop Dis* 2010; **4**: e689.
15 Stolfi C, Caruso R, Franze E, Sarra M, De Nitto D, Rizzo A *et al.* Interleukin-25 fails to activate STAT6 and induce alternatively activated macrophages. *Immunology* 2011; **132**: 66–77.
16 Bronte V, Zanovello P. Regulation of immune responses by L-arginine metabolism. *Nat Rev Immunol* 2005; **5**: 641–654.
17 Morris SM Jr. Arginine: beyond protein. *Am J Clin Nutr* 2006; **83**: 508S–512S.
18 Pearce EJ, MacDonald AS. The immunobiology of schistosomiasis. *Nat Rev Immunol* 2002; **2**: 499–511.
19 Wynn TA, Thompson RW, Cheever AW, Mentink-Kane MM. Immunopathogenesis of schistosomiasis. *Immunol Rev* 2004; **201**: 156–167.
20 Ahmed SF, Oswald IP, Caspar P, Hieny S, Keefer L, Sher A *et al.* Developmental differences determine larval susceptibility to nitric oxide-mediated killing in a murine model of vaccination against *Schistosoma mansoni*. *Infect Immun* 1997; **65**: 219–226.
21 Hesse M, Modolell M, La Flamme AC, Schito M, Fuentes JM, Cheever AW *et al.* Differential regulation of nitric oxide synthase-2 and arginase-1 by type 1/type 2 cytokines in vivo: granulomatous pathology is shaped by the pattern of L-arginine metabolism. *J Immunol* 2001; **167**: 6533–6544.
22 Allen JE, Wynn TA. Evolution of Th2 immunity: a rapid repair response to tissue destructive pathogens. *PLoS Pathog* 2011; **7**: e1002003.
23 Montoya JG, Liesenfeld O. Toxoplasmosis. *Lancet* 2004; **363**: 1965–1976.
24 Dubey JP. The history of *Toxoplasma gondii*–the first 100 years. *J Eukaryot Microbiol* 2008; **55**: 467–475.
25 Carme B, Demar M, Ajzenberg D, Darde ML. Severe acquired toxoplasmosis caused by wild cycle of *Toxoplasma gondii*, French Guiana. *Emerg Infect Dis* 2009; **15**: 656–658.
26 Wendte JM, Miller MA, Lambourn DM, Magargal SL, Jessup DA, Grigg ME. Self-mating in the definitive host potentiates clonal outbreaks of the apicomplexan parasites Sarcocystis neurona and *Toxoplasma gondii*. *PLoS Genet* 2010; **6**: e1001261.
27 Saeij JP, Boyle JP, Coller S, Taylor S, Sibley LD, Brooke-Powell ET *et al.* Polymorphic secreted kinases are key virulence factors in toxoplasmosis. *Science* 2006; **314**: 1780–1783.
28 Taylor S, Barragan A, Su C, Fux B, Fentress SJ, Tang K *et al.* A secreted serine-threonine kinase determines virulence in the eukaryotic pathogen *Toxoplasma gondii*. *Science* 2006; **314**: 1776–1780.
29 Saeij JP, Coller S, Boyle JP, Jerome ME, White MW, Boothroyd JC. *Toxoplasma* co-opts host gene expression by injection of a polymorphic kinase homologue. *Nature* 2007; **445**: 324–327.
30 Reese ML, Zeiner GM, Saeij JP, Boothroyd JC, Boyle JP. Polymorphic family of injected pseudokinases is paramount in *Toxoplasma* virulence. *Proc Natl Acad Sci USA* 2011; **108**: 9625–9630.
31 Rosowski EE, Lu D, Julien L, Rodda L, Gaiser RA, Jensen KD *et al.* Strain-specific activation of the NF-kappaB pathway by GRA15, a novel *Toxoplasma gondii* dense granule protein. *J Exp Med* 2011; **208**: 195–212.
32 Butcher BA, Fox BA, Rommereim LM, Kim SG, Maurer KJ, Yarovinsky F *et al. Toxoplasma gondii* rhoptry kinase ROP16 activates STAT3 and STAT6 resulting in cytokine inhibition and arginase-1-dependent growth control. *PLoS Pathog* 2011; **7**: e1002236.
33 Jensen KD, Wang Y, Wojno ED, Shastri AJ, Hu K, Cornel L *et al. Toxoplasma* polymorphic effectors determine macrophage polarization and intestinal inflammation. *Cell Host Microbe* 2011; **9**: 472–483.
34 Cheng W, Liu F, Li M, Hu X, Chen H, Pappoe F *et al.* Variation detection based on next-generation sequencing of type Chinese 1 strains of *Toxoplasma gondii* with different virulence from China. *BMC Genomics* 2015; **16**: 888.
35 Cai Y, Chen H, Mo X, Tang Y, Xu X, Zhang A *et al. Toxoplasma gondii* inhibits apoptosis via a novel STAT3-miR-17-92-Bim pathway in macrophages. *Cell Signal* 2014; **26**: 1204–1212.

36 Livak KJ, Schmittgen TD. Analysis of relative gene expression data using real-time quantitative PCR and the 2(-Delta Delta C (T)) Method. *Methods* 2001; **25**: 402–408.
37 Ding AH, Nathan CF, Stuehr DJ. Release of reactive nitrogen intermediates and reactive oxygen intermediates from mouse peritoneal macrophages. Comparison of activating cytokines and evidence for independent production. *J Immunol* 1988; **141**: 2407–2412.
38 Mantovani A, Locati M. Orchestration of macrophage polarization. *Blood* 2009; **114**: 3135–3136.
39 Garcia L, Hernandez I, Sandoval A, Salazar A, Garcia J, Vera J *et al.* Pirfenidone effectively reverses experimental liver fibrosis. *J Hepatol* 2002; **37**: 797–805.
40 Chu D, Du M, Hu X, Wu Q, Shen J. Paeoniflorin attenuates *schistosomiasis japonica*-associated liver fibrosis through inhibiting alternative activation of macrophages. *Parasitology* 2011; **138**: 1259–1271.
41 Gryseels B, Polman K, Clerinx J, Kestens L. Human schistosomiasis. *Lancet* 2006; **368**: 1106–1118.
42 Wynn TA, Cheever AW. Cytokine regulation of granuloma formation in schistosomiasis. *Curr Opin Immunol* 1995; **7**: 505–511.
43 Reiman RM, Thompson RW, Feng CG, Hari D, Knight R, Cheever AW *et al.* Interleukin-5 (IL-5) augments the progression of liver fibrosis by regulating IL-13 activity. *Infect Immun* 2006; **74**: 1471–1479.
44 Friedman SL. Liver fibrosis—from bench to bedside. *J Hepatol* 2003; **38**(Suppl 1): S38–S53.
45 Anthony B, Allen JT, Li YS, McManus DP. Hepatic stellate cells and parasite-induced liver fibrosis. *Parasit Vectors* 2010; **3**: 60.
46 Chang J, Hisamatsu T, Shimamura K, Yoneno K, Adachi M, Naruse H *et al.* Activated hepatic stellate cells mediate the differentiation of macrophages. *Hepatol Res* 2013; **43**: 658–669.
47 Krausgruber T, Blazek K, Smallie T, Alzabin S, Lockstone H, Sahgal N *et al.* IRF5 promotes inflammatory macrophage polarization and TH1-TH17 responses. *Nat Immunol* 2011; **12**: 231–238.
48 Mantovani A, Sica A, Sozzani S, Allavena P, Vecchi A, Locati M. The chemokine system in diverse forms of macrophage activation and polarization. *Trends Immunol* 2004; **25**: 677–686.
49 Mantovani A. From phagocyte diversity and activation to probiotics: back to Metchnikoff. *Eur J Immunol* 2008; **38**: 3269–3273.
50 Hoffmann KF, James SL, Cheever AW, Wynn TA. Studies with double cytokine-deficient mice reveal that highly polarized Th1- and Th2-type cytokine and antibody responses contribute equally to vaccine-induced immunity to Schistosoma mansoni. *J Immunol* 1999; **163**: 927–938.
51 Kaplan MH, Whitfield JR, Boros DL, Grusby MJ. Th2 cells are required for the *Schistosoma mansoni* egg-induced granulomatous response. *J Immunol* 1998; **160**: 1850–1856.
52 Fallon PG, Richardson EJ, McKenzie GJ, McKenzie AN. Schistosome infection of transgenic mice defines distinct and contrasting pathogenic roles for IL-4 and IL-13: IL-13 is a profibrotic agent. *J Immunol* 2000; **164**: 2585–2591.
53 Herbert DR, Holscher C, Mohrs M, Arendse B, Schwegmann A, Radwanska M *et al.* Alternative macrophage activation is essential for survival during schistosomiasis and downmodulates T helper 1 responses and immunopathology. *Immunity* 2004; **20**: 623–635.
54 Fallowfield JA, Mizuno M, Kendall TJ, Constandinou CM, Benyon RC, Duffield JS *et al.* Scar-associated macrophages are a major source of hepatic matrix metalloproteinase-13 and facilitate the resolution of murine hepatic fibrosis. *J Immunol* 2007; **178**: 5288–5295.
55 Murray PJ. Macrophages as a battleground for *toxoplasma* pathogenesis. *Cell Host Microbe* 2011; **9**: 445–447.
56 Biswas SK, Mantovani A. Macrophage plasticity and interaction with lymphocyte subsets: cancer as a paradigm. *Nat Immunol* 2010; **11**: 889–896.
57 Zhu J, Xu Z, Chen X, Zhou S, Zhang W, Chi Y *et al.* Parasitic antigens alter macrophage polarization during *Schistosoma japonicum* infection in mice. *Parasit Vectors* 2014; **7**: 122.
58 Barron L, Wynn TA. Fibrosis is regulated by Th2 and Th17 responses and by dynamic interactions between fibroblasts and macrophages. *Am J Physiol Gastrointest Liver Physiol* 2011; **300**: G723–G728.
59 Robben PM, Mordue DG, Truscott SM, Takeda K, Akira S, Sibley LD. Production of IL-12 by macrophages infected with *Toxoplasma gondii* depends on the parasite genotype. *J Immunol* 2004; **172**: 3686–3694.
60 Song E, Ouyang N, Horbelt M, Antus B, Wang M, Exton MS. Influence of alternatively and classically activated macrophages on fibrogenic activities of human fibroblasts. *Cell Immunol* 2000; **204**: 19–28.
61 Elsharkawy AM, Oakley F, Mann DA. The role and regulation of hepatic stellate cell apoptosis in reversal of liver fibrosis. *Apoptosis* 2005; **10**: 927–939.
62 Higashiyama R, Inagaki Y, Hong YY, Kushida M, Nakao S, Niioka M *et al.* Bone marrow-derived cells express matrix metalloproteinases and contribute to regression of liver fibrosis in mice. *Hepatology* 2007; **45**: 213–222.
63 Bogdan C. Nitric oxide and the immune response. *Nat Immunol* 2001; **2**: 907–916.
64 Noel W, Raes G, Hassanzadeh Ghassabeh G, De Baetselier P, Beschin A. Alternatively activated macrophages during parasite infections. *Trends Parasitol* 2004; **20**: 126–133.
65 Hesse M, Cheever AW, Jankovic D, Wynn TA. NOS-2 mediates the protective anti-inflammatory and antifibrotic effects of the Th1-inducing adjuvant, IL-12, in a Th2 model of granulomatous disease. *Am J Pathol* 2000; **157**: 945–955.